

Development of a new phasor measurement algorithm with decaying DC offset removal

Eugeniusz ROSOŁOWSKI^{✉*}

Wrocław University of Science and Technology, Wybrzeże Wyspiańskiego 27, 50-370 Wrocław, Poland

Abstract. Current and voltage phasors remain the basis of most power system protection and automation functions. Most phasor measurement algorithms used for this purpose are derived from the discrete Fourier transform (DFT) method, which is justified by its relatively simple implementation and good harmonic rejection. Growing requirements for faster relay operation and higher accuracy impose new conditions, particularly the need for a shorter measurement window and immunity to a decaying DC (DDC) component. To address these demands, new solutions are emerging, often based on algorithms with an expanding measurement window and on assumed definitions of the proposed measurement model. The method presented in this paper combines the properties of the DFT with a suitably modified least squares (LS) method to meet the expected requirements, ensuring fast estimation of the phasor components of the fundamental-frequency component while remaining insensitive to the presence of the DDC component. The attached results of simulation studies show details of the application and some of the properties of the method proposed.

Keywords: decaying DC component; digital filter; discrete Fourier transform; least error squares method; notch filter; phasor measurement; short circuit; variable window filter.

1. INTRODUCTION

Most algorithms used in AC networks for relay protection and automation purposes are still based on fast measurement of the orthogonal components of the current and voltage phasors. Most algorithms used for this purpose are derived from the discrete Fourier transform (DFT) method, which is justified by its relatively simple implementation, as well as its good harmonic interference filtering properties [1]. The growing need for faster processing and higher accuracy imposes new conditions, particularly the need for a shorter measurement window and higher resistance to interference in the form of a decaying DC component (DDC). For decades, different methods have been proposed to reduce the effect of the exponentially decaying component on the precision of estimating the amplitude and phase of the current fundamental component [2, 3]. An analysis of recent publications in this field shows that this issue remains an unresolved problem [4–6]. The proposed methods focus on finding effective ways to suppress elements in the form of DDC components by filtering out or capturing this interference in a signal model. This approach has a limited effect because of the theoretically unlimited spectrum of the exponentially decaying DC component (DDC).

There are several methods of eliminating interference in the form of an exponentially decaying DC component when we apply a measurement window longer than the period of the fundamental component of the signal. However, in many practical

applications, these algorithms do not meet modern requirements in terms of speed and accuracy. In response to this challenge, various methods have emerged, based on the idea of an expanding measurement window [7–9]. The advantage of this approach is that a stable phasor can be obtained even for a measurement window of less than half a period of the fundamental frequency component [8]. For phasor measurements with elimination of DDC interference, this approach supports the use of a recursive algorithm, significantly expanding its practical use [10, 11]. Unfortunately, the recursive implementation of the algorithm always raises problems with its stability.

An essential element of these methods is the estimation of the DDC time constant. Different methods were proposed, depending mainly on the length of the measurement window. The algorithm proposed in [10] calculates this parameter as the quotient of the shifted combination of complex phasor samples. Four consecutive samples are needed to determine the value searched. The phasor components can be calculated according to an algorithm with a fixed or an expanding measurement window. The authors of [5] propose a method based on a combination of current samples and shifted by a defined period, which leads to a quadratic equation with an unknown value of the time constant. Additional calculations are performed to determine the appropriate position of the selected samples in the waveform.

The authors of the paper [12] propose an interesting approach, consisting of modifying the classical DFT algorithm by considering the presence of DDC, as well as the deviation of the signal frequency from its nominal value. This modification is called the smart discrete Fourier transform (SDFT). However, the algorithm appears to be burdened with an excessive number of tasks, resulting in increased sensitivity of the proposed method to noise, necessitating additional smoothing.

*e-mail: eugeniusz.rosolowski@pwr.edu.pl

Manuscript submitted 2025-09-18, revised 2025-09-18, initially accepted for publication 2025-12-04, published in March 2026.

In paper [13], another algorithm is proposed to eliminate the effect of DDC on measuring the phasor component. The authors propose an algorithm with an expanding measurement window, which is initiated when a short circuit is detected. In subsequent expanding windows, accurate phasor values are calculated from three samples of the modified DFT algorithm. The algorithm is applied to high-speed distance protection relays.

The algorithm proposed below is created based on the DFT algorithm and the method of modified least squares. A preliminary idea of this approach was presented in the conference paper [9]. The estimator signal model is based on the oscillatory components of the observed signal, while the exponentially decaying constant component is treated as a disturbance, the parameters of which are identified in parallel with the process of measuring the basic parameters of the signal. Analogous to the well-known weighted least squares (WLS) method, the disturbance is represented in the form of a weight matrix. The method of determining this matrix and its contribution to the final form of the calculation procedure is a key element of the proposed method.

The remainder of the article is divided into the following sections. Section 2 discusses the principle of creating the proposed algorithm using a simple example of a signal model consisting of the phasor of the fundamental harmonic disturbed by the DDC component. In the next section, the method for removing the DDC component is presented. Section 4 presents an original generalization of the algorithm, with a detailed description of the application in the state with an expanding measurement window (transition state) and with a moving window (steady state of the algorithm), when the measurement window reaches the period length of the fundamental component of the signal. Section 5 includes an example illustrating how to apply the proposed algorithm, with some of its properties shown. The conclusions and a list of references are given at the end of the article.

2. MODIFIED LS ALGORITHM

When considering the task of estimating the fundamental harmonic current or voltage phasor, a signal model is usually defined consisting of a set of oscillatory components and the exponentially decaying DC component [2, 5, 9]:

$$y(k) = \sum_{j=1}^{L_n} Y_j \cos(n_j \alpha k + \varphi_j) - Y_a r^{k-1} + \varepsilon(k), \quad (1)$$

where $\alpha = 2\pi/N$ – angle between samples performed N times in a period $T_1 = 1/f_1$ (system frequency); n_j – coefficient determining the frequency of the oscillatory component j -th considered, for example, $n_1 = 1$ for the fundamental component; φ_j – phase of the considered component; L_n – number of oscillatory components considered; $r = \exp(b)$, $b = -T_1/(NT_a)$ – parameter representing the DC component with time constant T_a and initial magnitude Y_a ; Y_j – magnitude of the oscillatory component considered; k is the number counted from the onset of the disturbance in the form of the DDC component; $\varepsilon(k)$ – represents the signal components not included in the model and the measurement noise.

The main problem in designing an effective algorithm to eliminate the DDC component in a signal represented by model (1) is the quick and stable estimation of the decaying time constant of this component, which is expressed by the parameter r . In the case of full-cycle algorithms, the symmetry of the oscillatory components can be used for this purpose: summing samples of the signal (1) over one period of the waveform gives direct insight into the value of the searched DDC component [1, 2, 5, 7]. This approach can be extended to half-periodic algorithms with some loss of their frequency properties [4, 14]. The well-known principle applies here: shortening the measurement window leads to a faster assessment of the value of the parameter sought, but it also requires considering the impact of interference on this measurement [4].

Analyzing the signal model (1), it is easy to see that its symmetry, resulting from the presence of oscillatory components in the first part of the equation, is disturbed by the DDC element present in the second component, which has completely different properties. This alteration of the symmetry of the considered model is the source of the modification of the standard least squares (LS) method [9], which is the basis for the synthesis process of the appropriate algorithm presented in this paper.

2.1. Outline of the proposed method

The goal of this investigation is to find a successful algorithm that determines the parameters of the oscillatory component of the model (1). For this purpose, the LS method is proposed to derive a correlation algorithm with an expanding measurement window [9]. The derivation of the complete algorithm for model (1) is quite complex; therefore, to clarify the principles of the method used, it is proposed to simplify the process by starting with a signal model with only one oscillatory component, referring to the fundamental harmonic ($L_n = 1$, $n_1 = 1$) and the DDC component [9, 15]. For this case, model (1) can be represented in the following matrix form:

$$\mathbf{y}_{(M)}(k) = \mathbf{H}_{(M)}\mathbf{x}(k) + \varepsilon(k), \quad (2)$$

where $\mathbf{y}_{(M)}(k) = [y(k-M+1) \ y(k-M+2) \ \dots \ y(k)]^T$ – vector of input signal samples; M – the width of the measurement window: $M = M_0, M_0+1, \dots, N$; M_0 – minimal value of the width of the window; $\mathbf{x}(k)$ – estimates (outputs) defined in the data window M : $\mathbf{x}(k) = [x_c(k) \ x_s(k) \ x_a(k)]^T$ for $k \geq M_0$, with two orthogonal components: $x_c(k)$, $x_s(k)$, and $x_a(k)$, representing a magnitude of the DDC; $\varepsilon = [\varepsilon(k-M+1) \ \varepsilon(k-M+2) \ \dots \ \varepsilon(k)]^T$ – vector of measurement errors; index T means transposition; $\mathbf{H}_{(M)} = [\mathbf{h}_{c(M)} \ \mathbf{h}_{s(M)} \ \mathbf{h}_{a(M)}]$ – model parameters with column vectors:

$$\begin{aligned} \mathbf{h}_{c(M)} &= [h_c(1) \ h_c(2) \ \dots \ h_c(M)]^T, \\ \mathbf{h}_{s(M)} &= [h_s(1) \ h_s(2) \ \dots \ h_s(M)]^T, \\ \mathbf{h}_{a(M)} &= [h_a(1) \ h_a(2) \ \dots \ h_a(M)]^T, \end{aligned}$$

with: $h_c(j) = \cos((j-M)\alpha)$, $h_s(j) = -\sin((j-M)\alpha)$, $h_a(j) = -r^{(j-1)}$, $j = 1, 2, \dots, M$.

The LS estimator based on the 3-state model (2) is well known in the literature [1, 3]. Using simple transformations, the following nonrecursive estimator of the vector $\mathbf{x}(k)$ can be obtained:

$$\mathbf{x}(k) = \mathbf{P}_{(M)} \mathbf{H}_{(M)}^T \mathbf{y}_{(M)}(k), \quad (3)$$

with

$$\mathbf{P}_{(M)} = \left[\mathbf{H}_{(M)}^T \mathbf{H}_{(M)} \right]^{-1} = \begin{bmatrix} g_{11M} & g_{12M} & g_{13M} \\ g_{21M} & g_{22M} & g_{23M} \\ g_{31M} & g_{32M} & g_{33M} \end{bmatrix}^{-1}, \quad (4)$$

where elements g_{ijM} are functions of oscillatory components and unknown parameter r .

The main difficulty with the online application of estimator (3) arises from the need to invert matrix (4) in successive calculation steps, and, in addition, the parameter r must still be calculated. It should be noted here that the measurements conducted aim to determine the orthogonal phasor components of the fundamental harmonic of the signal, which form only a part of the vector \mathbf{x} (3). Having two components as in estimator (2), the estimated signal can be represented in the following complex form, which determines the signal phasor:

$$\underline{x}(k) = x_c(k) + jx_s(k). \quad (5)$$

For algorithms of the full period (when $M = N$), there are known methods to estimate the unknown DDC time constant T_a in the signal model (1) [1, 4]. Using the symmetry of the oscillatory components, this approach can be extended to the case of the half-periodic algorithm ($M = N/2$) after additional calculations [2, 4, 12]. However, a general online solution for $M < N$ and an unknown value of the time constant T_a (represented by the parameter r) must determine the coefficients of the matrix $\mathbf{P}_{(M)}$, which is not easy to provide for an online application. In the following section, an original method for modifying estimator (3) is presented, which allows the considered signal model to be reduced to a 2-state form while retaining its original properties, as in (2). The aim of these considerations is thus to obtain an estimator of the oscillatory components of the signal perturbed by the DDC component under the conditions of an expanding measurement window.

2.2. Modification of the LS algorithm

To simplify the procedure related to algorithm (3), it is proposed to reduce the estimator to only two states: $x_c(k)$ and $x_s(k)$ (3), keeping the features of the initial method. This can be done by eliminating the third equation in the matrix notation (3), and thus reducing the $\mathbf{P}_{(M)}$ matrix to dimension 2×2 . However, this operation should leave the relations pertaining to the first two equations unchanged. Thus, the calculated quantities: $x_c(k)$ and $x_s(k)$ remain unchanged. This can be achieved by zeroing out the coefficients: $g_{13M} = g_{23M} = 0$ in (4), shifting the results of the reduced relations to the first two columns of the matrix. The last row in this matrix can be removed because we are not interested in the direct calculation of the third component

$x_a(k)$ in the \mathbf{x} vector (2). This transformation is illustrated in (6) [7, 9]:

$$\mathbf{P}_{2(M)} = \begin{bmatrix} g_{11W} & g_{12W} & 0 \\ g_{21W} & g_{22W} & 0 \\ \sim & \sim & \sim \end{bmatrix}^{-1} = \begin{bmatrix} \mathbf{P}_{rF(M)}^{-1} & 0 \\ \sim & \sim & \sim \end{bmatrix}, \quad (6)$$

where $g_{11W} = g_{11M} - d_{rc(M)}$, $g_{12W} = g_{12M} - d_{rc(M)}$, $g_{21W} = g_{21M} - d_{rs(M)}$, $g_{22W} = g_{22M} - d_{rs(M)}$, with the coefficients $d_{rc(M)}$, $d_{rs(M)}$, which satisfy the following conditions: $g_{13M} - d_{rc(M)} = g_{23M} - d_{rs(M)} = 0$; the last row is omitted for further consideration.

It can be seen that the reduced matrix has the following form:

$$\mathbf{P}_{rF(M)} = \begin{bmatrix} g_{11W} & g_{12W} \\ g_{21W} & g_{22W} \end{bmatrix} = \left[\mathbf{H}_{rcs(M)}^T \mathbf{H}_{cs(M)} \right]^{-1}, \quad (7)$$

where $\mathbf{H}_{rcs(M)}^T = \left[\mathbf{H}_{cs(M)}^T - \mathbf{D}_{rcs(M)}^T \right]$, $\mathbf{H}_{cs(M)} = \left[\mathbf{h}_{c(M)} \quad \mathbf{h}_{s(M)} \right]$, and: $\mathbf{D}_{rcs(M)}^T = \mathbf{D}_{d(M)} \mathbf{1}_{2 \times M}$, with

$$\mathbf{D}_{d(M)} = \begin{bmatrix} d_{rc(M)} & 0 \\ 0 & d_{rs(M)} \end{bmatrix}, \quad \mathbf{1}_{2 \times M} = \begin{bmatrix} 1 & 1 & \dots & 1 \\ 1 & 1 & \dots & 1 \end{bmatrix}.$$

Finally, the estimator (3) takes the following form:

$$\mathbf{x}(k) = \mathbf{P}_{rF(M)} \mathbf{H}_{rcs(M)}^T \mathbf{y}_{(M)}(k) = \mathbf{G}_{r(M)}^T \mathbf{y}_{(M)}(k). \quad (8)$$

The estimator obtained (8) represents two digital filters whose coefficients are placed in two rows of the matrix $\mathbf{G}_{r(M)}^T$. After the provided transformations, the reduced estimator is still consistent with the LS procedure because it can be represented in the familiar form of the weighted LS algorithm [9]:

$$\mathbf{x}(k) = \left[\mathbf{H}_{cs(M)}^T \mathbf{W}_{(M)} \mathbf{H}_{cs(M)} \right]^{-1} \mathbf{H}_{cs(M)}^T \mathbf{W}_{(M)} \mathbf{y}_{(M)}(k), \quad (9)$$

where $\mathbf{W}_{(M)} = \left[\mathbf{H}_{cs(M)}^T \right]_{\text{right}}^{-1} \left[\mathbf{H}_{cs(M)}^T - \mathbf{D}_{rcs(M)}^T \right]$ – weight matrix and $\left[\mathbf{H}_{cs(M)}^T \right]_{\text{right}}^{-1}$ – right inverse matrix of $\mathbf{H}_{cs(M)}^T$.

It should be noted that the resulting weight matrix $\mathbf{W}_{(M)}$ has a different meaning here than in the classical weighted LS method, where it is a diagonal matrix with positive coefficients, the value of which reflects the degree of reliability of the associated measurements [16]. In contrast, in the case under consideration, the weight matrix is the result of the transformation of the initial measurement model (2) to a new form, as in (8), in which the number of states of the estimator is reduced due to shifting the exponentially decaying disturbance to the weight matrix.

The application of the above transformation needs to define the coefficients $d_{rc(M)}$, $d_{rs(M)}$, which lead to zero-related matrix elements: $g_{13W} = g_{23W} = 0$. In the proposed algorithm, the moving window technique is applied with expansion of this window width M in subsequent steps to reach the full period: $M = N$, [17, 18] (Fig. 1). Considering the coefficients of the vectors $\mathbf{h}_{c(M)}$, $\mathbf{h}_{s(M)}$ (2), the above condition gives the following

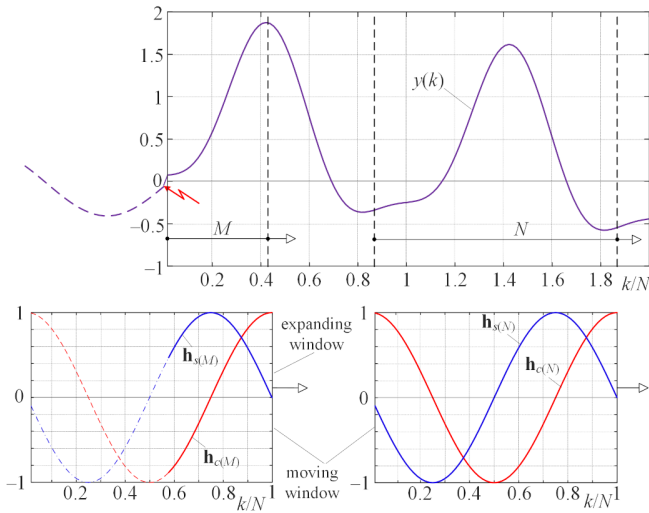


Fig. 1. Illustration of the expanding/moving window technique

relation with respect to the zero elements of the matrix $\mathbf{P}_{2(M)}$:

$$g_{13W} = \sum_{j=1}^M (\cos((j-M)\alpha) - d_{rc(M)}) r^{j-1} = 0, \quad (10)$$

$$g_{23W} = - \sum_{j=1}^M (\sin((j-M)\alpha) + d_{rs(M)}) r^{j-1} = 0,$$

from which one obtains:

$$d_{rc(M)} = p_{r(M)} ((r - \cos \alpha) c_{rM} + \sin \alpha \sin(M\alpha)), \quad (11)$$

$$d_{rs(M)} = p_{r(M)} (\sin \alpha c_{rM} - (r - \cos \alpha) \sin(M\alpha)),$$

with

$$p_{r(M)} = \frac{r-1}{(r^M - 1)(1 + r(r - 2\cos \alpha))}.$$

$$c_{rM} = r^M - \cos(M\alpha).$$

When the window reaches the length of the period: $M = N$, $k = N, N+1, \dots$, the above algorithm changes significantly. It is easy to see that the \mathbf{P}_{rF} matrix (7) takes a diagonal form, and the coefficients $d_{rc(M)} = d_{rc(N)}$, $d_{rs(M)} = d_{rs(N)}$ now strictly depend on the parameter r , which yields the following:

$$d_{rc(N)} = \frac{(r-1)(r - \cos \alpha)}{(1 + r(r - 2\cos \alpha))}, \quad (12)$$

$$d_{rs(N)} = \frac{(r-1) \sin \alpha}{(1 + r(r - 2\cos \alpha))}.$$

These relationships define the well-known full-period DDC component elimination algorithm [1, 7]. Similar relationships occur, although not as straightforwardly, for the half-period algorithm, confirming that the proposed method is an extension of the approach previously considered [14] to any measurement window width in the range $M > M_0$.

Returning to the estimator obtained in (8), it can be seen that it represents a pair of filters with an expanding measurement window ($M = M_0, M_0 + 1, \dots, N$), whose coefficients represent two rows of the matrix $\mathbf{G}_{r(M)}^T$:

$$\mathbf{G}_{r(M)}^T = \mathbf{P}_{rF(M)} \mathbf{H}_{rcs(M)}^T = \begin{bmatrix} \mathbf{g}_{rc(M)} \\ \mathbf{g}_{rs(M)} \end{bmatrix} \quad (13)$$

with

$$\mathbf{g}_{rc(M)} = [g_{rc}(1) \quad g_{rc}(2) \quad \dots \quad g_{rc}(M)],$$

$$\mathbf{g}_{rs(M)} = [g_{rs}(1) \quad g_{rs}(2) \quad \dots \quad g_{rs}(M)].$$

The above coefficients depend on an unknown time constant T_a (represented by the parameter r) and cannot be calculated directly. However, it is possible to gain insight into the structure of these coefficients by analyzing the $\mathbf{G}_{r(M)}^T$ matrix (13), which can be divided into two parts:

$$\mathbf{G}_{r(M)}^T = \mathbf{H}_{Fcs(M)}^T + \mathbf{G}_{rF(M)}^T = \begin{bmatrix} \mathbf{h}_{Fc(M)} + \mathbf{g}_{rFc(M)} \\ \mathbf{h}_{Fs(M)} + \mathbf{g}_{rFs(M)} \end{bmatrix}, \quad (14)$$

where $\mathbf{H}_{Fcs(M)}^T = (\mathbf{H}_{cs(M)}^T \mathbf{H}_{cs(M)})^{-1} \mathbf{H}_{cs(M)}^T$ is the coefficients matrix (two rows marked $\mathbf{h}_{Fc(M)}$ and $\mathbf{h}_{Fs(M)}$) of the standard Fourier algorithm with the increasing measurement window, while the matrix $\mathbf{G}_{rF(M)}^T$ defines two component filter coefficients (two rows marked $\mathbf{g}_{rFc(M)}$ and $\mathbf{g}_{rFs(M)}$), which can be considered as correction filters for the removal of the DDC component.

3. ALGORITHM FOR REMOVING DC COMPONENT

The modification of the LS algorithm defines a two-state phasor component filter (8) with the coefficient matrix (13). This matrix has extremely interesting properties: its separation according to (14) considerably simplifies the estimator (8). A proposed solution to this task is shown below.

3.1. Selection of oscillatory components

Based on (14), filter (8) can be split into two parts:

$$\mathbf{x}(k) = \mathbf{H}_{Fcs(M)}^T \mathbf{y}_{(M)}(k) + \mathbf{G}_{rF(M)}^T \mathbf{y}_{(M)}(k), \quad (15)$$

where the index M is changed to a constant value ($M = N$) when the algorithm reaches the full period window length (Fig. 1).

The first part of this filter is defined by the matrix $\mathbf{H}_{Fcs(M)}$ which does not depend on the parameter r and contains the coefficients of the standard 2-state Fourier filter with an expanding window [17, 18]:

$$\mathbf{x}_{Fcs}(k) = \mathbf{H}_{Fcs(M)}^T \mathbf{y}_{(M)}(k) = \begin{bmatrix} \mathbf{h}_{Fc(M)} \\ \mathbf{h}_{Fs(M)} \end{bmatrix} \mathbf{y}_{(M)}(k), \quad (16)$$

where $\mathbf{x}_{Fcs}(k) = \begin{bmatrix} x_{Fc}(k) \\ x_{Fs}(k) \end{bmatrix}$; the components of $\mathbf{H}_{Fcs(M)}^T$ can be easily calculated for the consecutive window M (14):

$$\mathbf{h}_{Fc(M)} = \begin{bmatrix} h_{Fc}(1) & h_{Fc}(2) & \cdots & h_{Fc}(M) \end{bmatrix},$$

$$\mathbf{h}_{Fs(M)} = \begin{bmatrix} h_{Fs}(1) & h_{Fs}(2) & \cdots & h_{Fs}(M) \end{bmatrix},$$

$$h_{Fc(M)}(j) = p_{a(M)} \cos((j-M)\alpha) - p_{b(M)} \cos((j-1)\alpha),$$

$$h_{Fs(M)}(j) = -p_{a(M)} \sin((j-M)\alpha) - p_{b(M)} \sin((j-1)\alpha),$$

for $j = 1, 2, \dots, M$; $M = M_0, M_0+1, \dots, N$, with

$$p_{a(M)} = \frac{2M \sin^2 \alpha}{M^2 \sin^2 \alpha - \sin^2(\alpha M)},$$

$$p_{b(M)} = \frac{2 \sin \alpha \sin(\alpha M)}{M^2 \sin^2 \alpha - \sin^2(\alpha M)},$$

when the full period is reached, the above coefficients take the form of the scaled coefficients of the full period filters:

$$\begin{aligned} \mathbf{h}_{Fc(N)} &= 2\mathbf{h}_{c(N)}/N = \{2 \cos((j-N)\alpha)/N\}, \\ \mathbf{h}_{Fs(N)} &= 2\mathbf{h}_{s(N)}/N = \{-2 \sin((j-N)\alpha)/N\}, \end{aligned} \quad (17)$$

where $j = 1, 2, \dots, N$; vectors $\mathbf{h}_c, \mathbf{h}_s$ are as in (2) for $M = N$.

The components obtained from the filter (16) are consistent with the desired orthogonal components of the fundamental harmonic phasor if the measured signal is not disturbed by the suppressed aperiodic component. In the opposite case, these components can deviate far from the expected values, and adequate correction is needed.

3.2. Selection of DDC component

The required correction is given by the second part of the filter (15), which represents the following two-element vector:

$$\mathbf{x}_{\Delta cs}(k) = \mathbf{G}_{rF(M)}^T \mathbf{y}_{(M)}(k) = \begin{bmatrix} \mathbf{g}_{rFc(M)} \\ \mathbf{g}_{rFs(M)} \end{bmatrix} \mathbf{y}_{(M)}(k), \quad (18)$$

where $\mathbf{x}_{\Delta cs}(k) = \begin{bmatrix} x_{\Delta rc}(k) \\ x_{\Delta rs}(k) \end{bmatrix}$; $\mathbf{G}_{rF(M)}^T$ matrix (15) can be presented in the following form:

$$\mathbf{G}_{rF(M)}^T = \mathbf{P}_{rF(M)} \mathbf{D}_{rcs(M)}^T \left[\mathbf{H}_{cs(M)} \mathbf{H}_{Fcs(M)}^T - \mathbf{I} \right]. \quad (19)$$

The matrix $\mathbf{G}_{rF(M)}^T$ (19) has crucial practical properties that become apparent when it is written in a slightly modified form. Substituting $\mathbf{D}_{rcs(M)}^T$ (7) in (19), we can obtain the following:

$$\mathbf{G}_{rF(M)}^T = \mathbf{P}_{rF(M)} \mathbf{D}_{d(M)} \mathbf{Q}_{cs(M)}^T, \quad (20)$$

where both rows of $\mathbf{Q}_{cs(M)}^T$ matrix (20) are identical:

$$\mathbf{Q}_{cs(M)}^T = (\mathbf{1}_{2 \times M} \mathbf{H}_{cs(M)}) \mathbf{H}_{Fcs(M)}^T - \mathbf{1}_{2 \times M} = \begin{bmatrix} \mathbf{g}_{cs(M)} \\ \mathbf{g}_{cs(M)} \end{bmatrix}, \quad (21)$$

with $\mathbf{q}_{cs(M)} = \begin{bmatrix} q_{cs}(1) & q_{cs}(2) & \cdots & q_{cs}(M) \end{bmatrix}$, which does not depend on the parameter r .

The bracketed multiplication in (21) is equivalent to summing the elements of the matrix vectors:

$$\mathbf{1}_{2 \times M} \mathbf{H}_{cs(M)} = \begin{bmatrix} \mathbf{1}_{1 \times M} \\ \mathbf{1}_{1 \times M} \end{bmatrix} \begin{bmatrix} \mathbf{h}_c(M) & \mathbf{h}_s(M) \end{bmatrix}, \quad (22)$$

where $\mathbf{h}_c(M), \mathbf{h}_s(M)$ (2) are column vectors with coefficients that adequately represent samples of cosine and sine functions:

$$\mathbf{1}_{1 \times M} \mathbf{h}_c(M) = \sum_{j=1}^M \cos((j-M)\alpha) \text{ for the direct component and}$$

$$\mathbf{1}_{1 \times M} \mathbf{h}_s(M) = -\sum_{j=1}^M \sin((j-M)\alpha) \text{ for the quadrature component.}$$

For the 2-state algorithm considered, the coefficients of the vector $\mathbf{q}_{cs(M)}$ (21) can be reduced to the simple form of the cosine function with modified magnitude and shifted angle:

$$q_{cs(M)}(j) = Q_{(M)} \cos(\alpha(j - (M+1)/2) - 1), \quad (23)$$

$$\text{where } Q_{(M)} = \frac{4 \sin(M\alpha/2) \cos(\alpha/2)}{M \sin \alpha + \sin(M\alpha)}.$$

Coefficients (23) can be used to filter the input signal in the following form:

$$y_{q0}(k) = \mathbf{q}_{cs(M)} \mathbf{y}_{(M)}(k) = \sum_{j=1}^M q_{cs(M)}(j) y(k - M + j). \quad (24)$$

Filter (24) has noteworthy properties: it is generally a low-pass notch-type filter, cutting out the fundamental frequency components and attenuating the higher frequency components (Fig. 2). Furthermore, it should be noted that the filtering considered is part of the procedure implemented by the estimator (18). The impulse function of the filter changes with the expanding data window according to (21). Due to these properties, the output signal $y_{q0}(k)$ (24) is deprived of the fundamental harmonic and some other oscillatory components (depending on the width of the window M) and therefore, can be used to determine the

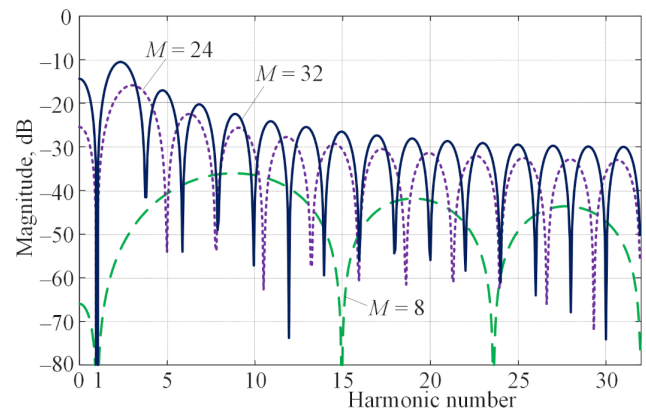


Fig. 2. Magnitude characteristics of the filter (24) for the width of the selected measurement window, $N = 64$

parameter r of the DDC component [9]. For an online application, the filter coefficients (23) can be calculated offline and memorized.

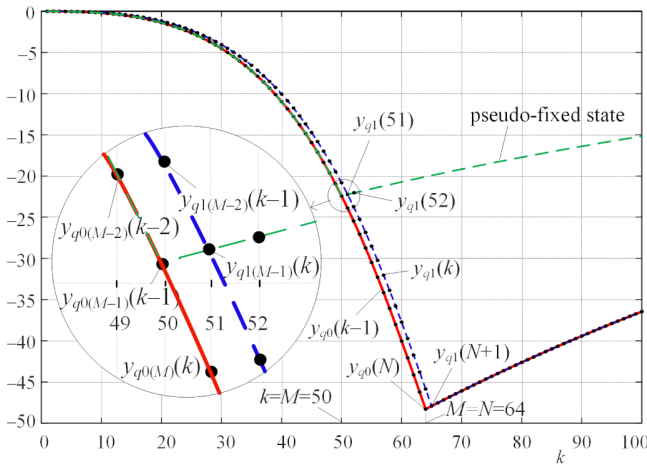


Fig. 3. Signal $y_{q0}(k)$ in the transient and steady state period (solid line), and the pseudo-fixed state (dashed line: $y_{q1}(k)$); DC time constant $T_a = 0.04$ s, $N = 64$, $X_1 = 1.2$, $X_a = 0.6$, Equation (1)

The presence of a notch-type filter in this algorithm to suppress interference components can be promising, as confirmed in a slightly different configuration in the work [19]. In this case, the notch-type filter also removes the fundamental component, making the filtering result primarily an interfering aperiodic component. For the signal model considered (1), the output waveform is shown in Fig. 3 (solid line). In the transient state of the algorithm, the measurement window M is extended until the set length is reached ($M = N$). In the example considered, a full period filter (24) is used, whose transient lasts for $N = 64$ s/p, after which the response represents a signal proportional to the waveform of the DDC component in the input signal. It can be seen that the magnitude of the signal $y_{q0}(k)$ is exceedingly small at the beginning of the transient and increases as the measurement window widens. This is a consequence of the filter frequency response (24), which is strongly attenuated for a short window (Fig. 2). Figure 3 shows the signal waveform in the first period of the algorithm with an expanding measurement window ($k = 1, \dots, N$) and then for the algorithm with a moving window ($k > N$) – a solid line representing the waveform proportional to the DDC disturbance. Similarly, the twin signal $y_{q1}(k+1)$ can be obtained as in (24) with the same impulse vector $\mathbf{q}_{cs(M)}$ but with the input signal vector shifted by one: ($k+1$) as in (25):

$$\begin{aligned}
 y_{q1}(k+1) &= \mathbf{q}_{cs(M)} \mathbf{y}_{(M)}(k+1) \\
 &= \sum_{j=1}^M q_{cs(M)}(j) y(k-M+j+1). \quad (25)
 \end{aligned}$$

It is interesting to note that the pair of such twinning samples $y_{q0}(k)$, $y_{q1}(k+1)$ is located on a curve that is locally proportional to the exponentially decaying constant component defined in model (1) [9] (named the pseudo-fixed state in Fig. 3). This

property can be directly used to calculate the parameter r . After ordering the indices with respect to the current discrete time, the following relation is obtained:

$$r = \frac{y_{q1}(k)}{y_{q0}(k-1)}, \quad k = M_0, M_0+1, \dots, N \quad (26)$$

where $M_0 = 3$ for the 3-state algorithm as in (3).

The waveform defined by $y_{q1}(k)$ is twinned with the waveform $y_{q0}(k-1)$, which can be seen in Fig. 3 (thin dashed line in the enlarged part). The way these ‘twin’ runs are calculated is specific to the proposed method, so let us write down how these waveforms are created in a more accessible form:

$$\begin{aligned}
 y_{q0}(k-1) &= q_{cs(M-1)}(1)y(1) + q_{cs(M-1)}(2)y(2) \\
 &\quad + \dots + q_{cs(M-1)}(M-1)y(k-1), \\
 y_{q1}(k) &= q_{cs(M-1)}(1)y(2) + q_{cs(M-1)}(2)y(3) \\
 &\quad + \dots + q_{cs(M-1)}(M-1)y(k). \quad (27)
 \end{aligned}$$

It is seen that both signals are obtained from the same length as the $M-1$ impulse function, but with a shifted set of input signals. To clarify the complicated indexing of the variables in the above expressions, the designations of the corresponding quantities are shown in the enlarged part in Fig. 3 for the transient period of the algorithm. The numerical quantities (0, 1) in the index distinguish between twin runs, M is the length of the measurement window, $k = M$ for $k < N$ (the transition state of the algorithm), and $M = N$ for $k \geq N$ (steady state). It can be seen that the designation in the length index of the measurement window: (M), ($M-1$), etc., can be omitted without loss of information. Figure 3 also shows the steady-state waveform for the case when an algorithm with a measurement window of 50 samples is used (instead of a full period, $N = 64$). This waveform is labeled the pseudo-fixed state. In this case, the measurement window expands to $M = 50$, and then the algorithm switches to a moving window mode. Both waveforms overlap when the algorithm reaches the length of the measurement window equal to the prescribed period ($M = N$ for the full period algorithm or any other adopted value).

The example in Fig. 3 shows how the procedure regarded can be used to create algorithms with a transition state length different from that of the full-period filter considered. It may be noted that due to close values in the numerator and denominator of (26), the estimator considered is sensitive to interferences contained in the input signal, especially for a short measurement window. Therefore, particular attention should be paid to the determination of the parameter r . The primary way to reduce the errors considered is to adequately smooth out the input signal $y(k)$, which can be achieved by additional digital filtering [9] or by reducing the cutoff frequency of the analogue antialiasing filters. Another way is to smooth the waveform of the calculated values of the parameter r . However, it would not be expected to obtain a stable algorithm response for a dynamic network in less than about 15% of the fundamental harmonic period with a distorted input signal coming from the high-voltage grid.

It may be seen that the procedure for determining the r parameter is based on matrix $\mathbf{Q}_{cs(M)}^T$ (21). The completion of the

filtering procedure (24) in the form of (18) follows from the structure of matrix (20), and the inclusion of the first two matrix factors leads to the following form of estimator (18):

$$\begin{bmatrix} x_{\Delta rc}(k) \\ x_{\Delta rs}(k) \end{bmatrix} = \begin{bmatrix} h_{rc(M)} \\ h_{rs(M)} \end{bmatrix} y_{q0}(k), \quad (28)$$

where

$$\begin{bmatrix} h_{rc(M)} \\ h_{rs(M)} \end{bmatrix} = \mathbf{P}_{rF(M)} \begin{bmatrix} d_{rc(M)} \\ d_{rs(M)} \end{bmatrix}. \quad (29)$$

The unexpected form of the right-hand side (29) follows from the fact that both rows of matrix $\mathbf{Q}_{cs(M)}^T$ (21) are equal (diagonal quadratic matrix $\mathbf{D}_{d(M)}$ (7) can be reduced to a vector matrix (29)). The scaling coefficients $h_{rc(M)}$, $h_{rs(M)}$ (29) depend on the parameter r . For the online procedure, they can be calculated offline and stored in computer memory. As can be seen, this must be done for different window lengths M and different values of the parameter r . A suitable interpolation procedure can be used to reproduce these factors online from stored values.

The result of these deductions is an algorithm for measuring the phasor components of the fundamental harmonic of a signal with an expanding measurement window. The general form of the algorithm is given in (15). To determine the second component of the estimator (15) (correction components (18)), the value of the parameter r (26) must be calculated in parallel in the following steps.

Once the algorithm reaches a measurement window length equal to the period of the fundamental harmonic ($M = N$), it undergoes some modification: the filters (16) coefficients are set according to (17), and all coefficients (23) bring constant values: $q_{cs(N)}(j) = -1$, $j = 1, 2, \dots, N$. This procedure takes the form of an algorithm with a fixed window $M = N$.

4. IMPROVEMENT OF THE BASIC ALGORITHM

A certain inconvenience of this algorithm is the way to calculate the correction components $x_{\Delta rc}(k)$ and $x_{\Delta rs}(k)$, which are functions of the parameter r . Moreover, the transient quantities determining the components (29) change with the expanding measurement window. To improve the algorithm, it is proposed to extend the application of the algorithm with 'twin' runs (27) to both components on the right-hand side of the estimator (15). Accordingly, including the results of twin filtering similarly to (27) in the notation of the correction signals (24) yields the following cosine component samples:

$$\begin{aligned} x_{\Delta rc0}(k-1) &= h_{rc(M-1)} \sum_{j=1}^{M-1} q_{cs(M-1)}(j) y(k-M+j), \\ x_{\Delta rc1}(k) &= h_{rc(M-1)} \sum_{j=1}^{M-1} q_{cs(M-1)}(j) y(k-M+j+1), \end{aligned} \quad (30)$$

and adequately for the quadrature components. The same principle is applied to obtain the pair of twin signals representing

the fundamental components $x_{Fc}(k)$, $x_{Fs}(k)$ in (16):

$$\begin{aligned} x_{Fc0}(k-1) &= \sum_{j=1}^{M-1} h_{Fc(M-1)}(j) y(k-M+j), \\ x_{Fc1}(k) &= \sum_{j=1}^{M-1} h_{Fc(M-1)}(j) y(k-M+j+1), \end{aligned} \quad (31)$$

and analogously for quadrature components. The interrelationship of the variables in (31) is similar to that of filters (27), as explained in Fig. 3. Note that, as a general rule, the twin pairs of waveforms (30) and (31) are the results of filtering with the same impulse functions, $g_{cs(M-1)}$, and $h_{Fc(M-1)}$, respectively. The vectors representing these functions expand when going to the next sample (expanding measurement window), which makes it possible to write:

$$x_{\Delta rc0}(k) = h_{rc(M)} y_{q0}(k), \quad (32)$$

$$x_{Fc0}(k) = \mathbf{h}_{Fc(M)} \mathbf{y}(M)(k) \quad (33)$$

as the first parts of the next twinning waveforms. Applying the expressions (30)–(33), the following relations can be created based on (15):

$$x_{c0}(k-1) = x_{Fc0}(k-1) + h_{rc(M-1)} y_{q0}(k-1), \quad (34)$$

$$x_{c1}(k) = x_{Fc1}(k) + h_{rc(M-1)} y_{q1}(k), \quad (35)$$

$$x_{c0}(k) = x_{Fc0}(k) + h_{rc(M)} y_{q1}(k),$$

which can also be easily repeated for quadrature components. It can be verified that the last two equations (35) represent estimators of the same quantity, which is the direct orthogonal component of the measured signal: $x_{c1}(k) = x_{c0}(k) = x_c(k)$. Similarly, one can obtain: $x_{s1}(k) = x_{s0}(k) = x_s(k)$. Thus, based on (35) (and considering similar relations for the quadrature components), we obtain:

$$\begin{aligned} h_{rc(M)} &= (h_{rc(M-1)} y_{q1}(k) + x_{Fc1}(k) - x_{c0}(k)) / y_{q0}(k), \\ h_{rs(M)} &= (h_{rs(M-1)} y_{q1}(k) + x_{Fs1}(k) - x_{s0}(k)) / y_{q0}(k). \end{aligned} \quad (36)$$

The recursive relationships in the above equations with respect to the h_{rc} and h_{rs} functions can be easily removed by using the relations defined above and the known relationship between samples of the fundamental frequency components:

$$\begin{bmatrix} x_c(k-1) \\ x_s(k-1) \end{bmatrix} = \begin{bmatrix} \cos \alpha & \sin \alpha \\ -\sin \alpha & \cos \alpha \end{bmatrix} \begin{bmatrix} x_c(k) \\ x_s(k) \end{bmatrix}.$$

Substituting $h_{rc(M-1)}$ from (34) into (36) (and making it similar to $h_{rs(M-1)}$), considering the relationship (26), after obvious transformations, leads to the following system of equations with

two unknowns ($h_{rc(M)}, h_{rs(M)}$):

$$\begin{aligned} y_{q0}(k-1)y_{q0}(k)(h_{rc(M)}b_c(k) - h_{rs(M)}b_s(k)) \\ = x_c(k) - x_{Fc0}(k)b_s(k), \\ y_{q0}(k-1)y_{q0}(k)(h_{rs(M)}b_c(k) + h_{rc(M)}b_s(k)) \\ = x_s(k) - x_{Fs0}(k)b_c(k), \end{aligned} \quad (37)$$

where

$$\begin{aligned} b_c(k) &= y_{q0}(k-1) - y_{q1}(k) \cos \alpha, \\ b_s(k) &= y_{q1}(k) \sin \alpha, \end{aligned} \quad (38)$$

$$v_c(k) = y_{q0}(k-1)x_{Fc1}(k) - y_{q1}(k)x_{Fc0}(k-1), \quad (39)$$

$$v_s(k) = y_{q0}(k-1)x_{Fs1}(k) - y_{q1}(k)x_{Fs0}(k-1). \quad (40)$$

The solution of (37) gives the following expressions:

$$\begin{aligned} h_{rc(M)} &= (x_c(k) - x_{Fc0}(k)) / y_{q0}(k), \\ h_{rs(M)} &= (x_s(k) - x_{Fs0}(k)) / y_{q0}(k), \end{aligned} \quad (41)$$

where

$$\begin{aligned} x_c(k) &= \frac{v_c(k)b_c(k) + v_s(k)b_s(k)}{b_c^2(k) + b_s^2(k)}, \\ x_s(k) &= \frac{v_s(k)b_c(k) - v_c(k)b_s(k)}{b_c^2(k) + b_s^2(k)}, \end{aligned} \quad (42)$$

which resolves the recursive dependence in (36) and gives a compact form of the desired component estimators (42).

The relations (42) present estimators of the fundamental harmonic phasor components of a signal represented by model (2). According to the derivation performed, algorithm (42) is initiated when a fault or other disturbance is detected in the supervised network, from which the index calculation begins: $k = M = 1$, and the sample collection starts in an ascending measurement window. For $k \geq M_0$, the measurement of the quantities appearing in (42) begins. According to (38)–(40), these are determined by pairs of waveforms: $x_{Fc1}(k) - x_{Fc0}(k-1)$, $x_{Fs1}(k) - x_{Fs0}(k-1)$ and $y_{q1}(k) - y_{q0}(k-1)$, which are the result of filtering of (31) and (27), respectively. In both cases, the pair of ‘twin’ filters has a length of $M - 1$ samples. As can be seen from the detailed equations, the pair of these filters is shifted by one sample in the expanding measurement window length of M samples. When the length of the measurement window exceeds one period: $k > N$, there is a transition to the fixed state of the algorithm, in which the indices k and M are separated: $M = N$ (fixed length of the measurement window), moving relative to the measured signal (Fig. 1). In the full-period algorithm with a moving measurement window, the coefficient vectors of the individual filters do not change. Consequently, the twin signals overlap since the filtering results in the k -th sample of both twin filters are identical.

The above description refers to the full-period algorithm with an expanding measurement window. It can be easily adapted to a different window length at which the steady-state transition occurs. This principle is illustrated in Fig. 3, where for $M = 50$

a transition to steady-state measurement occurs (pseudo-fixed-state curve). In this way, algorithms can be combined, for example, the half-period algorithm ($M = N/2$) that transforms into a full-period algorithm for $M = N$. In this case, the algorithm with the expanding window continues until the first part (half-period) of the measurement is complete.

5. SIMULATION TEST

Verification of the proposed algorithm was conducted on a model of the power system fragment as in Fig. 4. The model was developed using the ATP/EMTP program [20]. Several tests were performed with different system parameters, while the parameters of the example discussed further are as follows:

- Overhead line: $l = 250$ km, $R'_0 = 0.275$ Ω /km, $R'_1 = 0.0275$ Ω /km, $X'_0 = 1.027$ Ω /km, $X'_1 = 0.315$ Ω /km, $C'_0 = 8.5$ nF/km, $C'_1 = 13.0$ nF/km
- Both end systems: $\underline{E}_S = 400$ kV $\angle 49.5^\circ$, $\underline{Z}_{S0} = 2.334 + j22.5$ Ω , $\underline{Z}_{S1} = 1.3312 + j15.0$ Ω , $\underline{E}_R = 400$ kV $\angle -69.5^\circ$ with impedances as in system S ; system frequency $f_1 = 50$ Hz
- Fault AB at $m = 0.8$, $t_F = 0.02688$ s, $R_F = 0.1$ Ω
- Sampling frequency: $f_s = 3200$ Hz ($N = 64$ s/p), antialiasing filters in the form of the third-order RC scheme with cut-off frequency $f_c = 1000$ Hz
- The analyzed quantities are scaled to the primary side.

The phase current waveforms for the AB fault at a distance of 200 km from the substation S , recorded at this substation, are presented in Fig. 5. From these currents, the AB fault loop cur-

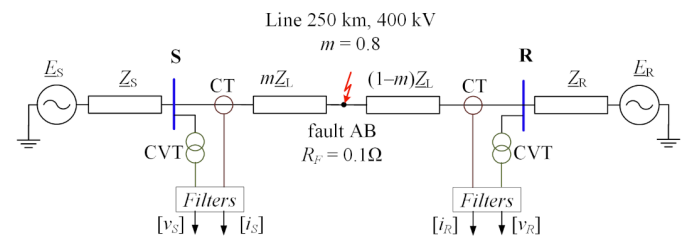


Fig. 4. Scheme of the model considered

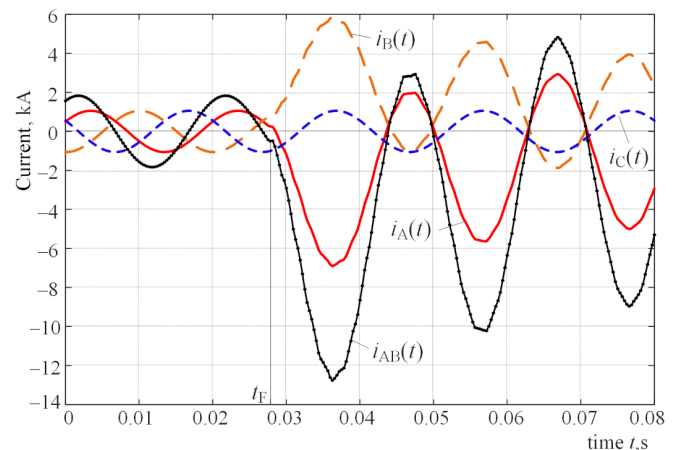


Fig. 5. Three-phase current waveforms obtained from the considered network model during the AB fault as seen from the substation S

rent was created: $i_{AB} = i_A - i_B$, which is the procedure input to the discussed signal input (Fig. 5, variable $i_{AB}(t)$). The algorithm started from $k = 3 = M_0$ after the inception of the fault.

The magnitude waveform of the first harmonic components obtained during the operation of the algorithm is presented in Fig. 6 (curve I_4). The intense transient immediately after a short circuit in the line deviates from the assumptions made in the signal model considered (1), which manifests itself in the form of large oscillations in the estimated signal. This phenomenon can be significantly reduced by appropriately suppressing interference in the input signal (for example, by lowering the cut-off frequency f_c of the antialiasing filter). It should be noted that the phase of the output signal (estimated first harmonic) is consistent with the phase of the input signal [9].

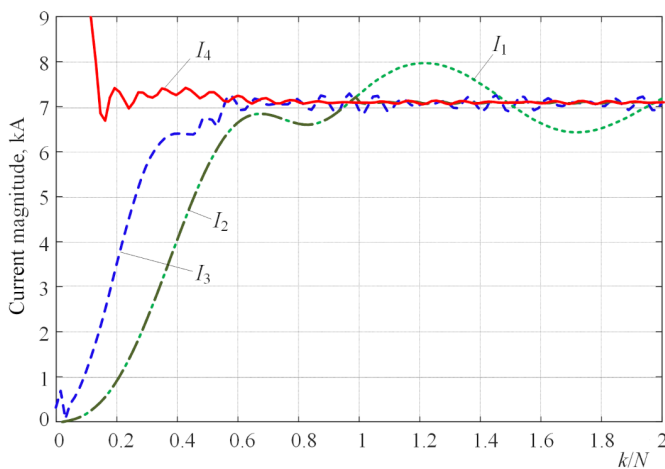


Fig. 6. Waveforms obtained during the algorithm operation at the substation S

For comparison, results of other estimators are also presented: standard full-period algorithm (I_1), full-period algorithm with rejection of DDC component (I_2), and half-period Fourier algorithm (I_3). The same results but for the measurement at the substation R are presented in Fig. 7. In this case, the distance to the fault site is 50 km.

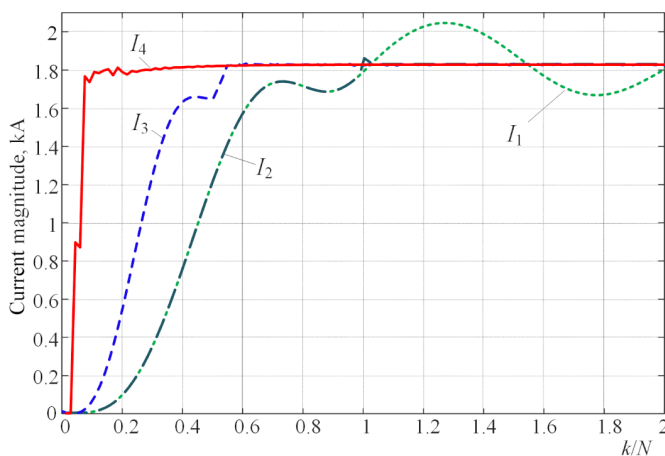


Fig. 7. Waveforms obtained for measurement at substation R

6. CONCLUSIONS

This paper presents an innovative approach to developing a robust algorithm for measuring the phasor of the fundamental components of the voltage and current waveforms disturbed by the decaying DC component. It was shown that the proposed modification of the well-known LS algorithm makes it possible to exploit the symmetries present in different models of the signals under consideration as oscillatory components and exponentially decaying DC components to separate them efficiently. Important tools in the proposed selection procedure are pairs of identical nonrecursive filters applied to the shifted input signals. Such filtering results in pairs of related (twin) signals, which are used for the separation of the signal components. It has been shown that a pair of filters with frequency characteristics that ensure the excision of the fundamental component of the signal (notch-type filter) can be used to determine the value of the decaying time constant of the interfering aperiodic component (represented by the parameter r). Similarly, pairs of filters used, derived from the standard algorithm DFT, also make it possible to determine the phasor components of the fundamental harmonic of the signal with full elimination of the interfering DDC component. Both procedures can be used in the form of an algorithm with an expanding measurement window, which ensures a stable measurement of the disturbed signal already from the length of the measurement window covering about 15% of the period of the fundamental component of the measured signal.

Once the increasing measurement window length is equal to the period of the fundamental harmonic of the signal, the algorithm takes the familiar form of a full-period Fourier algorithm with an additional procedure to eliminate DDC components.

An important distinguishing feature of the algorithm obtained is its fully analytical form, which suggests potential for extension to other disturbances occurring in the measured signal. This concerns the possibility of shaping the frequency response of the estimator (for both magnitude and phase) and considering several aperiodic disturbances. These aspects will be addressed in future work.

An example posted using a simulation model illustrates how to apply the described method and confirms its effectiveness compared to existing methods.

REFERENCES

- [1] A.G. Phadke and J.S. Thorp, *Computer relaying for power systems*. John Wiley & Sons Ltd, 2nd ed., pp. 163–166, 2009.
- [2] T.S. Sidhu, X. Zhang, F. Albasri, and M.S. Sachdev, “Discrete-Fourier-transform-based technique for removal of decaying dc offset from phasor estimates,” *Proc. Inst. Elect. Eng., Gen. Transm. Distrib.*, vol. 150, no. 6, pp. 745–752, 2003, doi: [10.1049/ip-gtd:20030943](https://doi.org/10.1049/ip-gtd:20030943).
- [3] M.S. Sachdev and M.A. Baribeau, “A new algorithm for digital impedance relays,” *IEEE Trans. Power Appl. Syst.*, vol. 98, pp. 2232–2240, 1979, doi: [10.1109/TPAS.1979.319422](https://doi.org/10.1109/TPAS.1979.319422).
- [4] T.S. Sidhu, X. Zhang, and V. Balamourougan, “A New Half-Cycle Phasor Estimation Algorithm,” *IEEE Trans. Power Del.*, vol. 20, no. 2, pp. 1299–1305, 2005, doi: [10.1109/TPWRD.2004.834677](https://doi.org/10.1109/TPWRD.2004.834677).
- [5] Y. Guo, M. Kezunovic, and D. Chen, “Simplified algorithms for removal of the effect of exponentially decaying DC-offset on the

- Fourier algorithm,” *IEEE Trans. Power Del.*, vol. 18, no. 3, pp. 711–717, 2003, doi: [10.1109/TPWRD.2003.813894](https://doi.org/10.1109/TPWRD.2003.813894).
- [6] A. Haji-Mohammadi, M. Sanaye-Pasand, and S.-A. Ahmadi, “Novel Method for Decaying DC Component Removal Based on Solving the Differential Equations,” *IEEE Trans. Power Del.*, vol. 40, no. 2, pp. 693–704, 2025, doi: [10.1109/TPWRD.2024.3516950](https://doi.org/10.1109/TPWRD.2024.3516950).
- [7] E. Rosolowski, J. Izykowski, and B. Kasztenny, “Adaptive measuring algorithm suppressing a decaying dc component for digital protective relays,” *Electr. Power Syst. Res.*, vol. 60, pp. 99–105, 2001, doi: [10.1016/S0378-7796\(01\)00171-7](https://doi.org/10.1016/S0378-7796(01)00171-7).
- [8] H. Hajizadeh, S.-A. Ahmadi, and M. Sanaye-Pasand, “An Analytical Fast Decaying DC Mitigation Method for Digital Relaying Applications,” *IEEE Trans. Power Del.*, vol. 36, no. 6, pp. 3529–3537, 2021, doi: [10.1109/TPWRD.2020.3044376](https://doi.org/10.1109/TPWRD.2020.3044376).
- [9] E. Rosolowski, “A New Method for Fast Removal of Decaying Offset in Relaying Input Current,” in *23rd International Scientific Conference on Electric Power Engineering (EPE)*, Brno, Czech Republic, May 2023, pp. 24–26, doi: [10.1109/EPE58302.2023.10149233](https://doi.org/10.1109/EPE58302.2023.10149233).
- [10] B.R. Kumar, A. Mohapatra, and S. Chakrabarti, “A Novel Sub-Cycle-Based Method for Estimation of Decaying DC Component and Fundamental Phasor,” in *IEEE Trans. Instrum. Meas.*, vol. 70, p. 9005410, 2021, doi: [10.1109/TIM.2021.3122199](https://doi.org/10.1109/TIM.2021.3122199).
- [11] S.R. Nam, J.M. Sohn, S.H. Kang, and J.K. Park, “Modified notch filter-based instantaneous phasor estimation for high-speed distance protection,” *Electr. Eng.*, vol. 89, pp. 311–317, 2007, doi: [10.1007/s00202-006-0006-6](https://doi.org/10.1007/s00202-006-0006-6).
- [12] J.Z. Yang and C.W. Liu, “Complete elimination of DC offset in current signals for relaying applications,” in *2000 IEEE Power Engineering Society Winter Meeting*, Singapore, 2000, vol. 3, pp. 1933–1938, doi: [10.1109/PESW.2000.847649](https://doi.org/10.1109/PESW.2000.847649).
- [13] C.S. Chen, C.W. Liu, and J.A. Jiang, “Application of combined adaptive Fourier filtering technique and fault detector to fast distance protection,” *IEEE Trans. Power Del.*, vol. 21, no. 2, pp. 619–626, 2006, doi: [10.1109/TPWRD.2005.858808](https://doi.org/10.1109/TPWRD.2005.858808).
- [14] E. Rosolowski, J. Izykowski, and B. Kasztenny, “A new half-cycle adaptive phasor estimator immune to the decaying DC component for digital protective relaying,” in *Proc. Thirty-Second Annual NAPS*, Waterloo, Canada, Oct. 2000, pp. 2:17–2:24.
- [15] H. Yu, Z. Jin, H. Zhang, and V. Terzija, “A phasor estimation algorithm robust to decaying DC component,” *IEEE Trans. Power Del.*, vol. 37, no. 2, pp. 860–870, 2022, doi: [10.1109/TPWRD.2021.3073135](https://doi.org/10.1109/TPWRD.2021.3073135).
- [16] K.S. Surana, *Numerical Methods and Methods of Approximation in Science and Engineering*. CRC Press, Taylor & Francis Group, 2019, pp. 311–342.
- [17] C.S. Chen, C.W. Liu, and J.Z. Yang, “A DC offset removal scheme with a variable data window for digital relaying,” in *Int. Conf. on Power Systems and Communications Infrastr. for the Future*, Beijing, Sept. 2002, doi: [10.1049/iet-gtd.2014.1150](https://doi.org/10.1049/iet-gtd.2014.1150).
- [18] B. Kasztenny, M.V. Mynam, T. Joshi, and C. Daniels, “A new digital filter using window resizing for protective relay applications,” in *15th Int. Conf. on DPSP*, Liverpool, UK, 9–12 Mar. 2020, pp. 1–6, doi: [10.1049/cp.2020.0053](https://doi.org/10.1049/cp.2020.0053).
- [19] J.K. Hwang, “Phasor Estimation with Finite Impulse Response Notch Filtering and Half-Cycle Discrete Fourier Transform,” in *IEEE Power & Energy Society General Meeting*, Chicago, USA, 16–20 July 2017, doi: [10.1109/PESGM.2017.8273952](https://doi.org/10.1109/PESGM.2017.8273952).
- [20] H.W. Dommel, S. Bhattacharya, V. Brandwajn, H.K. Lauw, and L. Martí, *Electromagnetic Transients Program Reference Manual (EMTP Theory Book)*, Bonneville Power Administration, USA, 1992.